Multitarget Antibacterial Efficacy of Green-Synthesized *Boerhavia diffusa* AgNPs: Molecular and In Silico Perspectives on MDR *Bacillus cereus*

Sasi Lekha. S[1*] , S. Antony[2]

1, Research Scholar, Reg.No: 20113082102008, Department of Microbiology, Malankara Catholic College, Mariagiri, Kaliyakavilai, Affiliated to Manonmaniam Sundaranar University, Tirunelveli, India.

2, Assistant Professor, Department of Microbiology, Malankara Catholic College, Mariagiri, kaliyakavilai, India.

ABSTRACT

The creation of environmentally friendly and sustainable antimicrobial substitutes is imperative due to the multidrug-resistant (MDR) bacteria's quick spread. In this work, an ethanolic extract of *Boerhavia diffusa* was used to biosynthesize silver nanoparticles (AgNPs). Quercetin and caffeic acid were found to be the main phytochemicals in charge of the stability and decrease of AgNPs by LC–MS profiling. The produced nanoparticles had a zeta potential of -23.8 mV and were spherical, crystalline, and stable, with an average size of 50–57 nm. Strong concentration-dependent inhibition against the MDR soil isolate *Bacillus cereus* (BR3) was shown by antibacterial testing. 99% similarity with *Bacillus cereus* and *Bacillus tropicus* was confirmed by molecular identification utilizing 16S rRNA gene sequencing. Additionally, quercetin's substantial binding affinities toward the important bacterial resistance enzyme Glycerophosphoryl diester phosphodiesterase (4R7O) were demonstrated by molecular docking study. The integrated experimental and computational findings suggest that *B. diffusa*–mediated AgNPs may serve as promising ecofriendly antimicrobial agents against resistant bacterial pathogens.

KEY WORDS: Multidrug resistance, *Boerhavia diffusa*, Nanoparticles, Green synthesis, Quercetin.

INTRODUCTION

The hunt for long-lasting and efficient antimicrobial treatments has accelerated due to the quick growth of multidrug-resistant (MDR) bacterial infections. *Bacillus cereus* is a prominent opportunistic bacteria among these pathogens that is linked to nosocomial infections and foodborne diseases. Promising substitutes are provided by nanobiotechnology, especially the environmentally friendly production of silver nanoparticles (AgNPs) from medicinal plants. The benefits of plant-mediated synthesis include its cost-effectiveness, environmental friendliness, and

the presence of bioactive phytochemicals that serve as stabilizing and reducing agents [10–13]. The manufacture of nanoparticles and therapeutic uses of *Boerhavia diffusa*, a well-known medicinal plant with proven antibacterial and antioxidant qualities, have been extensively investigated [14–18].

In order to guarantee precise taxonomic confirmation and bolster the dependability of subsequent experimental studies, the MDR isolate BR3 was molecularly identified in the current work using 16S rRNA gene sequencing. Molecular characterisation allows comparison with internationally reported MDR strains and offers accurate strain-level identification. Additionally, the interaction between phytochemical-capped AgNP-associated bioactive chemicals and important bacterial target proteins involved in metabolic control and membrane integrity was predicted using molecular docking analysis. By clarifying potential binding affinities and molecular inhibitory processes, this in silico method validates experimental results. Thus, a thorough foundation for comprehending the multitargeted antibacterial activity of *B. diffusa*-mediated AgNPs against MDR *Bacillus cereus* is provided by the combination of green nanotechnology, molecular identification, and molecular docking.

MATERIALS AND METHODS

Ethical Compliance

Plant material was collected in accordance with institutional and national biodiversity regulations [1].

Plant Extraction and LC–MS Profiling

In Tirunelveli, India, fresh *Boerhavia diffusa* plants were gathered. The substance was ground up and shade-dried. For twenty-four hours, ten grams of powder were continuously shaken in 100 milliliters of ethanol. To find reducing phytochemicals, the filtrate was put through LC–MS analysis (Waters SQD2 Q-TOF) in both positive and negative electrospray ionization modes (100–1200 m/z) [19,22].

Green Synthesis of Silver Nanoparticles

40 mL of 1 mM $AgNO_3$ and 8 mL of plant extract were combined to create AgNPs, which were then incubated at 150 rpm for 48 hours at room temperature [16,17]. A visual color shift served as preliminary confirmation of the nanoparticle formation, and UV-visible spectroscopy was used to track it.

Characterization of AgNPs

Several analytical methods were used to thoroughly analyze the produced silver nanoparticles. To track the creation of nanoparticles and validate the distinctive Surface Plasmon Resonance (SPR) peak of AgNPs, UV-visible spectroscopy (300–700 nm) was utilized [8]. Functional groups involved in the reduction and stabilization process were identified using Fourier Transform Infrared (FTIR) spectroscopy in the 400–4000 cm^{-1} range [20]. X-ray diffraction (XRD) analysis was used to ascertain the nanoparticles' crystalline constitution and phase structure [15]. Field Emission Scanning Electron Microscopy (FESEM) and Transmission Electron Microscopy (TEM) were used to analyze the morphological characteristics and particle size distribution [14]. Furthermore, the hydrodynamic diameter and colloidal stability of the produced nanoparticles were assessed using Zeta potential measurements and Dynamic Light Scattering (DLS) analysis [18].

MDR Screening and Antibacterial Assay

After being serially diluted, the bacterial isolates from pesticide-contaminated brinjal root soil were plated on nutrient agar and cultured for 24 hours at 37°C. The Kirby-Bauer disc diffusion method was used to evaluate purified colonies for antibiotic susceptibility [4]. Mueller-Hinton agar was covered with inocula adjusted to the 0.5 McFarland standard, followed by the application of twelve antibiotic discs. Zones of inhibition were assessed and multidrug-resistant (MDR) isolates were identified following a 24-hour incubation period. Bacillus cereus (BR3) was identified as the most resistant strain. Agar well diffusion was used to assess the antibacterial activity of the produced AgNPs [10]. 100 µL of AgNPs (20–80 µg/mL) were applied to 6 mm wells on inoculated plates. Zones of inhibition were noted during a 24-hour incubation period at 37°C. Every test was run in triplicate.

Molecular Identification and 16S rRNA Sequencing

A bacterial genomic DNA isolation kit was used to obtain genomic DNA from the chosen MDR isolates (BR1 and BR3). Under conventional PCR conditions, the 16S rRNA gene was amplified using universal primers 27F (5′-AGAGTTTGATCMTGGCTCAG-3′) and 1492R (5′-TACGGYTACCTTGTTACGACTT-3′) [36]. Commercial purification and sequencing were performed on amplified products (~1.5 kb). The NCBI BLAST tool was used to conduct sequence similarity searches [37]. To verify taxonomic identity, phylogenetic analysis was carried out using MEGA software and the neighbor-joining method [38].

Molecular Docking Analysis

The binding affinities of the discovered phytochemicals (quercetin, fumaric acid, ferulic acid, and gentisic acid) against bacterial target proteins linked to antibiotic resistance were assessed using molecular docking experiments. The Protein Data Bank provided the 3D crystal structures of β-lactamase 2 (PDB ID: 5FQB) and glycerophosphoryl diester phosphodiesterase (PDB ID: 4R7O). PubChem provided the ligand structures, which Chem3D was used to optimize. AutoDock Vina was used for docking simulations [39, 40]. LigPlot+ and Discovery Studio Visualizer were used to investigate molecular interactions and compute binding energies [41, 42].

RESULTS AND DISCUSSION

Phytochemical Profiling and Nanoparticle Formation

An obvious color shift from pale yellow to dark brown, signifying the reduction of Ag^{+} to Ag^{0}, provided preliminary confirmation of the creation of silver nanoparticles (Figure 1) [16]. Quercetin (m/z 290.27) and caffeic acid (m/z 205.32) were found to be the main phytochemicals in charge of the reduction and stabilization process by LC–MS profiling [22–24]. These chemicals' hydroxyl and carbonyl groups probably help with electron donation and nanoparticle surface capping. A clear Surface Plasmon Resonance (SPR) signal at 434.80 nm was visible in UV-Vis spectroscopy (Figure 1), which is indicative of uniformly distributed spherical AgNPs [8,9]. The phytochemical role in reduction and stabilization was confirmed by FTIR analysis, which revealed strong peaks at 3338, 2928, 1652, 1451, 1380, 1086, and 511 cm^{-1}, which corresponded to O–H, C–H, amide, and C–O functional groups [20,21]. XRD patterns (Figure 1) revealed characteristic diffraction peaks indexed to the (111), (200), and (220) planes, confirming a face-centered cubic (fcc) crystalline structure of silver [15]. The majority of the nanoparticles in the 50.28–57.78 nm range

were spherical, according to the FESEM and TEM pictures. Good colloidal stability was suggested by the Zeta potential value of −23.8 mV (Figure 1), which was probably caused by negatively charged phytoconstituents adhering to the nanoparticle surface [18]. Overall, the findings validate that *B. diffusa* successfully mediated the green production of solid, crystalline AgNPs.

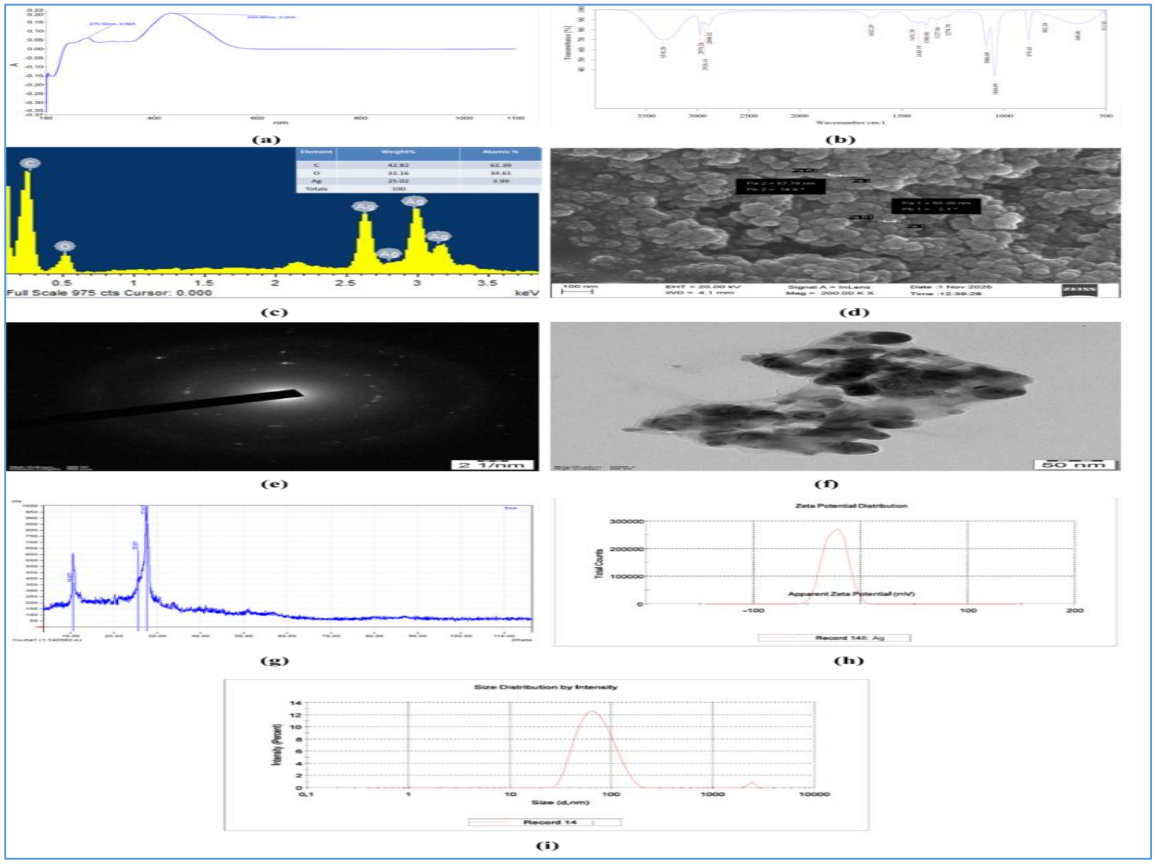

Fig. 1. *Characterization of B.diffusa mediated Silver nanoparticles by (a) UV- Vis Spectrophotometric analysis; (b) FTIR analysis; (c) EDX analysis; (d) FE-SEM; (e) Selected Area Electron Diffraction; (f) TEM analysis; (g) XRD analysis; (h) and (i) DLS analysis*

Antibacterial activity

The synthesized AgNPs exhibited strong concentration-dependent antibacterial activity against multidrug-resistant *Bacillus cereus* (BR3), as shown in Figure 2. At 60 µg/mL, a maximal zone of inhibition of 16 mm was observed, indicating strong bactericidal activity. The dose-responsive character of plant-mediated AgNPs is highlighted by the progressive increase in inhibition diameter with concentration, which also confirms earlier findings on their efficacy against resistant Gram-positive bacteria [10–13,30–35]. Nanoparticle adhesion to the bacterial membrane,

membrane integrity rupture, and subsequent intracellular component leaking are probably the causes of the antibacterial effect [11,12].

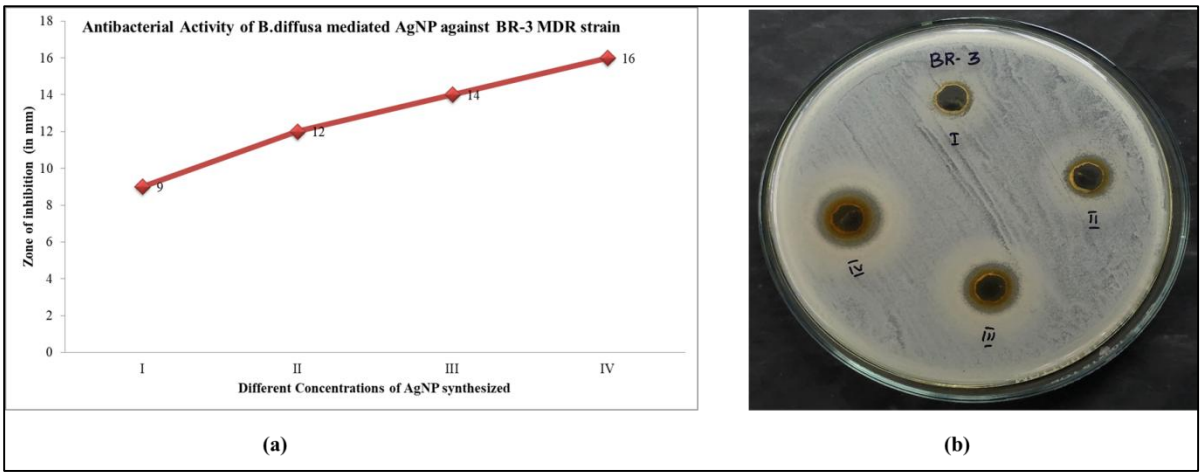

Fig 2. *Showing the Concentration Dependent Antibacterial Activity of B.diffusa Mediated AgNPs against MDR strain (BR-3) from Pesticide Treated Brinjal Root Soil* ***(a)*** *Line graph showing concentration-dependent increase in the zone of inhibition.* ***(b)*** *Agar well diffusion plate displaying inhibition zones at four AgNP concentrations.*

**BR- Code given to the isolates; I–IV correspond to increasing AgNP concentrations of 10, 20, 40, and 60 µg,*

Furthermore, cellular dysfunction may result from the release of Ag^+ ions interfering with essential metabolic and enzymatic functions [10–13]. This study's constant negative zeta potential (−23.8 mV) and moderate particle size (50–57 nm) probably improved nanoparticle–cell interactions and prolonged antibacterial efficacy. Overall, the results (Figure 2) demonstrate that *B. diffusa*–mediated AgNPs serve as effective and ecofriendly antimicrobial agents against MDR strains [30–35].

Molecular Identification and 16S rRNA Sequencing

16S rRNA gene amplification yielded an amplicon of about 1,500 bp, confirming the MDR isolate BR3. Its taxonomic identity was confirmed by BLAST analysis, which showed >99% sequence similarity with Bacillus cereus strains in the NCBI database. Close clustering with known MDR *B. cereus* strains was shown by phylogenetic analysis, indicating that genetic characteristics linked to virulence and resistance are conserved. After being submitted to GenBank, the sequence was

given an accession number. The reliability of BR3 as an MDR model for assessing nanoparticle-mediated antibacterial processes is strengthened by the use of 16S rRNA sequencing, which offers precise species-level identification because of conserved and hypervariable areas [36–40].

Molecular Docking

The interaction between a few chosen phytochemicals linked to *Boerhavia diffusa* and important bacterial target proteins was assessed using molecular docking research. Table 1 provides an overview of the hydrogen bond interactions, binding affinities, and active site residues that contribute to ligand stabilization. Strong inhibitory potential was shown by the data, which showed persistent ligand–protein complexes and favorable binding energies. The docked complexes' visualization (Fig. 3a–d) showed that the ligands were precisely positioned within the active pockets, with strong hydrogen bonding and hydrophobic interactions involving catalytic residues. These interactions imply disruption of the proteins in charge of metabolic control, enzymatic function, and membrane integrity. The robust binding patterns bolster a multitarget inhibitory mechanism that enhances oxidative stress and membrane disruption brought on by AgNP.

According to previous findings, bioactive chemicals originating from plants demonstrate efficient binding to vital bacterial enzymes, hence augmenting antimicrobial activity [41–45]. Thus, molecular-level evidence for the increased antibacterial activity of *B. diffusa*-mediated AgNPs against MDR *Bacillus cereus* is provided by the docking results shown in Table 1 and Fig. 3a–d.

Table 1: Docking results of ligands with Glycerophosphoryl diester phosphodiesterase (PDB ID: 4R7O)

Ligand	Interacting Residues	Types of Interactions
Quercetin	ASP256, TRP212, TYR280, LEU210, PHE190, HIS43, GLN188, GLU70, GLU152, ASP72, HIS85, ARG44, PHE300, THR281	Van der Waals, conventional H-bonds (ASP256, ASP72, GLU70, GLU152), pi–cation, pi–anion, pi–alkyl
Fumaric acid	GLU70, GLU152, GLN188, ASP72, HIS43, HIS85, PHE300, TYR280, PHE190, ARG44	Conventional H-bonds (GLU70, GLU152, ASP72, ARG44), van der Waals (PHE190, LEU210, TYR280, PHE300)

Ferulic acid	GLU70, GLU152, GLN188, PHE190, ARG44, HIS43, HIS85, TYR280, LEU210, PHE300	H-bonds (GLU70, GLU152), pi–cation (HIS85), pi–alkyl (HIS43, TYR280), van der Waals
Gentisic acid	ARG254, ASP287, THR281, TRP212, ASP256, LEU253, ASN	Conventional H-bonds (ARG254, ASP287), pi–alkyl (THR281), van der Waals

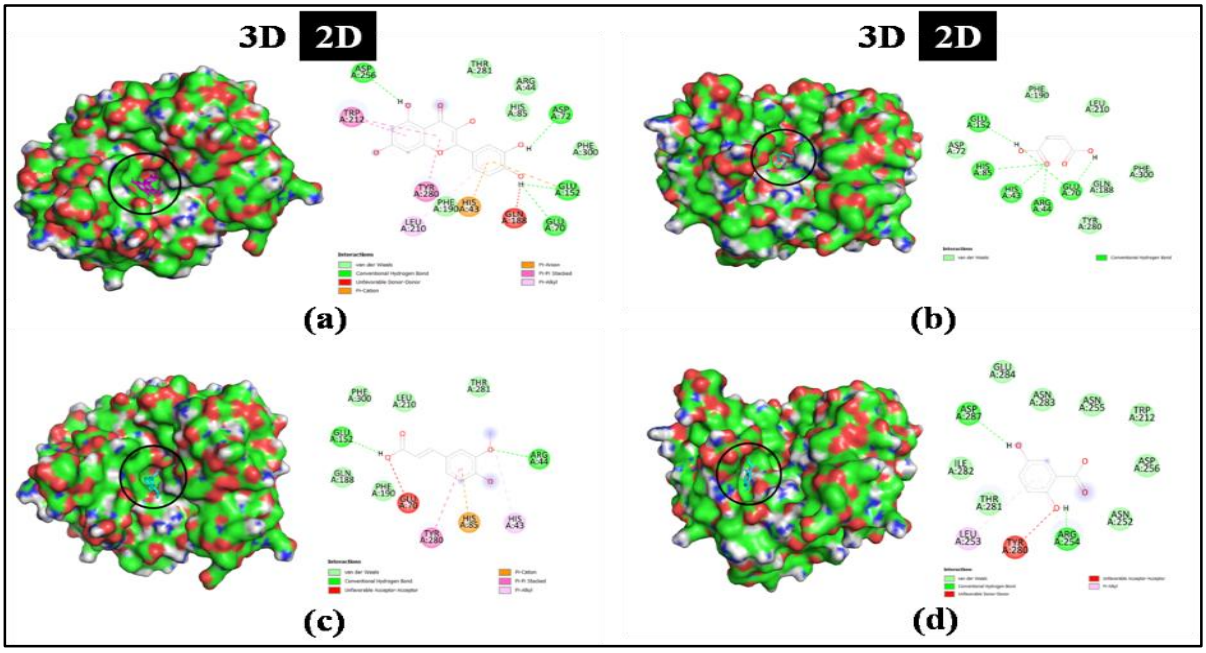

Fig. 3. 3D and 2D interaction of Glycerophosphoryl diester phosphodiesterase (PDB 4R7O) and (a) - quercetin, (b) - fumaric acid, (c) - ferulic acid, and (d) - gentisic acid.

CONCLUSION

To sum up, the green-synthesised silver nanoparticles (AgNPs) from *Boerhavia diffusa* shown strong antibacterial activity against multidrug-resistant (MDR) *Bacillus cereus* (BR3) that was dependent on concentration. The isolate's taxonomic identity was validated by molecular identification using 16S rRNA sequencing, confirming its usage as a therapeutically relevant MDR model. Strong ligand–protein interactions and multitarget suppression of crucial bacterial proteins involved in membrane integrity and metabolic control were shown by mechanistic insights derived from proteomic analysis and molecular docking. The synergistic activity of phytochemical-capped AgNPs is highlighted by the combined actions of enzyme inhibition, oxidative stress generation, and membrane disruption. Overall, the potential of *B. diffusa*-mediated AgNPs as environmentally

benign and efficient substitutes for controlling MDR *Bacillus cereus* and similar resistant infections is highlighted by our combined experimental and In silico approach.

REFERENCES

1. World Health Organization. *Antimicrobial Resistance: Global Report on Surveillance 2014.* Geneva: WHO Press; 2014.
2. Ventola CL. The antibiotic resistance crisis: part 1: causes and threats. *Pharm Ther.* 2015;40(4):277–283.
3. O'Neill J. *Tackling Drug-Resistant Infections Globally: Final Report and Recommendations.* London: Review on Antimicrobial Resistance; 2016.
4. Davies J, Davies D. Origins and evolution of antibiotic resistance. *Microbiol Mol Biol Rev.* 2010;74(3):417–433.
5. Blair JMA, Webber MA, Baylay AJ, Ogbolu DO, Piddock LJV. Molecular mechanisms of antibiotic resistance. *Nat Rev Microbiol.* 2015;13(1):42–51.
6. Laxminarayan R, Duse A, Wattal C, Zaidi AKM, Wertheim HFL, Sumpradit N, et al. Antibiotic resistance—the need for global solutions. *Lancet Infect Dis.* 2013;13(12):1057–1098.
7. Prestinaci F, Pezzotti P, Pantosti A. Antimicrobial resistance: a global multifaceted phenomenon. *Pathog Glob Health.* 2015;109(7):309–318.
8. Rai M, Yadav A, Gade A. Silver nanoparticles as a new generation of antimicrobials. *Biotechnol Adv.* 2009;27(1):76–83.
9. Pal S, Tak YK, Song JM. Does the antibacterial activity of silver nanoparticles depend on the shape of the nanoparticle? *Appl Environ Microbiol.* 2007;73(6):1712–1720.
10. Morones JR, Elechiguerra JL, Camacho A, Holt K, Kouri JB, Ramírez JT, Yacaman MJ. The bactericidal effect of silver nanoparticles. *Nanotechnology.* 2005;16(10):2346–2353.
11. Feng QL, Wu J, Chen GQ, Cui FZ, Kim TN, Kim JO. A mechanistic study of the antibacterial effect of silver ions on *Escherichia coli* and *Staphylococcus aureus. J Biomed Mater Res.* 2000;52(4):662–668.
12. Kim JS, Kuk E, Yu KN, Kim JH, Park SJ, Lee HJ, et al. Antimicrobial effects of silver nanoparticles. *Nanomedicine.* 2007;3(1):95–101.
13. Sondi I, Salopek-Sondi B. Silver nanoparticles as antimicrobial agent: a case study on *E. coli. J Colloid Interface Sci.* 2004;275(1):177–182.
14. Iravani S. Green synthesis of metal nanoparticles using plants. *Green Chem.* 2011;13(10):2638–2650.
15. Ahmed S, Ahmad M, Swami BL, Ikram S. A review on plants extract mediated synthesis of silver nanoparticles. *J Adv Res.* 2016;7(1):17–28.
16. Shankar SS, Rai A, Ahmad A, Sastry M. Rapid synthesis of Au, Ag, and bimetallic nanoparticles using neem extract. *J Colloid Interface Sci.* 2004;275(2):496–502.

17. Song JY, Kim BS. Rapid biological synthesis of silver nanoparticles using plant leaf extracts. *Bioprocess Biosyst Eng.* 2009;32(1):79–84.
18. Gurunathan S, Kalishwaralal K, Vaidyanathan R, Deepak V, Pandian SRK, Muniyandi J, et al. Biosynthesis, purification and characterization of silver nanoparticles. *Colloids Surf B Biointerfaces.* 2009;74(1):328–335.
19. Harborne JB. *Phytochemical Methods: A Guide to Modern Techniques of Plant Analysis.* 3rd ed. London: Chapman & Hall; 1998.
20. Coates J. Interpretation of infrared spectra, a practical approach. In: Meyers RA, editor. *Encyclopedia of Analytical Chemistry.* Chichester: Wiley; 2000. p. 10815–10837.
21. Kumar V, Yadav SK. Plant-mediated synthesis of silver and gold nanoparticles and their applications. *J Nanobiotechnol.* 2018;16:84.
22. Singh A, Singh PK, Tiwari RK. Phytochemical and pharmacological profile of *Boerhavia diffusa. J Ethnopharmacol.* 2012;144(1):1–15.
23. Rawat AKS, Mehrotra S, Tripathi SC, Shome U. Hepatoprotective activity of *Boerhavia diffusa* roots. *Phytochemistry.* 1997;45(1):113–116.
24. Apu AS, Liza MS, Jamaluddin ATM, Howlader MA, Saha RK, Rizwan F, et al. Pharmacological activities of *Boerhavia diffusa:* a review. *Pharmacogn Rev.* 2012;6(11):59–66.
25. Mittal AK, Chisti Y, Banerjee UC. Synthesis of metallic nanoparticles using plant extracts. *J Colloid Interface Sci.* 2013;415:39–46.
26. Prabhu S, Poulose EK. Silver nanoparticles: mechanism of antimicrobial action. *Int Nano Lett.* 2012;2:32.
27. Li WR, Xie XB, Shi QS, Duan SS, Ouyang YS, Chen YB. Antibacterial effect of silver nanoparticles on *Staphylococcus aureus. Appl Microbiol Biotechnol.* 2010;85(4):1115–1122.
28. Franci G, Falanga A, Galdiero S, Palomba L, Rai M, Morelli G, Galdiero M. Silver nanoparticles as potential antibacterial agents. *Molecules.* 2015;20(5):8856–8874.
29. Clinical and Laboratory Standards Institute (CLSI). *Performance Standards for Antimicrobial Susceptibility Testing.* 28th ed. Wayne, PA: CLSI; 2018.
30. Baker C, Pradhan A, Pakstis L, Pochan DJ, Shah SI. Synthesis and antibacterial properties of silver nanoparticles. *J Nanosci Nanotechnol.* 2005;5(2):244–249.
31. Lara HH, Ayala-Núñez NV, Ixtepan-Turrent L, Rodríguez-Padilla C. Mode of antiviral action of silver nanoparticles. *Nanotechnology.* 2010;21:145101.
32. Zhang XF, Liu ZG, Shen W, Gurunathan S. Silver nanoparticles: synthesis and antibacterial mechanisms. *Int J Mol Sci.* 2016;17(9):1534.
33. Durán N, Durán M, de Jesus MB, Seabra AB, Fávaro WJ, Nakazato G. Silver nanoparticles: a new view on mechanistic aspects. *J Nanobiotechnol.* 2016;14:16.
34. Shrivastava S, Bera T, Roy A, Singh G, Ramachandrarao P, Dash D. Characterization of enhanced antibacterial effects of silver nanoparticles. *Nanotechnology.* 2007;18:225103.

35. Kalishwaralal K, BarathManiKanth S, Pandian SRK, Deepak V, Gurunathan S. Silver nanoparticles impede bacterial growth. *Colloids Surf B Biointerfaces.* 2010;79(2):340–344.
36. Marchesi JR, Sato T, Weightman AJ, et al. Design and evaluation of useful bacterium-specific PCR primers. *Appl Environ Microbiol.* 1998;64:795–799.
37. Altschul SF, Gish W, Miller W, Myers EW, Lipman DJ. Basic local alignment search tool. *J Mol Biol.* 1990;215:403–410.
38. Kumar S, Stecher G, Li M, Knyaz C, Tamura K. MEGA X: Molecular evolutionary genetics analysis. *Mol Biol Evol.* 2018;35:1547–1549.
39. Morris GM, Huey R, Lindstrom W, et al. AutoDock4 and AutoDockTools4. *J Comput Chem.* 2009;30:2785–2791.
40. Trott O, Olson AJ. AutoDock Vina: improving speed and accuracy of docking. *J Comput Chem.* 2010;31:455–461.
41. Laskowski RA, Swindells MB. LigPlot+: multiple ligand–protein interaction diagrams. *J Chem Inf Model.* 2011;51:2778–2786.
42. BIOVIA Discovery Studio Visualizer v21. Dassault Systèmes; 2021.
43. Brem J, Cain R, Cahill S, et al. Structural basis of metallo-β-lactamase inhibition. *Nat Commun.* 2016;7:12406.
44. Behbood L, et al. Quercetin as a potential β-lactamase inhibitor: molecular insights. *J Biomol Struct Dyn.* 2024.
45. Nesme J, Simonet P. The soil resistome. *ISME J.* 2015;9:2426–2437.